



OPEN Echocardiographic assessment of left atrial structural and functional changes after catheter ablation in paroxysmal atrial fibrillation with preserved ejection fraction

Qi Zhang, Nan Nan Liu✉, Jing Shu Sun, Zu Lu Wang, Ming Liang, Gui Shen Li & Mei Yi Wang

To evaluate dynamic changes in left atrial (LA) structure and function after catheter ablation in paroxysmal atrial fibrillation (PAF) patients with preserved ejection fraction using conventional echocardiography and 2D speckle-tracking imaging (2D-STI). Eighty-nine PAF patients underwent echocardiography at 48 h pre-ablation, 1-day, 1-month, and 3-month post-ablation. Parameters included LA diameter (LAD), volume index (LAVI), strain (left atrial systolic strain (LASRs), early left atrial diastolic strain (LASRe), late left atrial diastolic strain (LASRa), and stiffness (LAsT). At 1 day post-ablation, left ventricular ejection fraction (LVEF), peak early LA diastolic strain (LASRe), peak late LA diastolic strain (LASRa), and their strain rates were lower than baseline, while LA ejection fraction (LAEF) was higher (all $P < 0.05$). At 1 month and 3 months post-ablation, LA diameter (LAD), end-systolic/diastolic volumes, and volume index (LAVI) were significantly reduced, while left atrial appendage flow velocity (LAA-V), LAEF, LVEF, peak LA systolic strain (LASRs), and related strain rates were increased (all $P < 0.05$). Cox regression analysis showed that the 1-month LASRs recovery rate (Δ LASRs) was an independent predictor of AF recurrence (hazard ratio = 0.72, 95% confidence interval: 0.54–0.96, $P = 0.023$). After catheter ablation, LA reverse remodeling exhibits a pattern of “functional recovery preceding structural recovery”. The improvement in functional parameters at 1 month post-ablation is of significant value for predicting long-term prognosis.

Keywords Paroxysmal atrial fibrillation, Catheter ablation, Echocardiography, Two-dimensional speckle tracking imaging, Left atrium

Atrial fibrillation (AF), the most prevalent cardiac arrhythmia, has emerged as a global health challenge. AF not only impairs patients' quality of life but also significantly heightens the risks of stroke, heart failure, and all-cause mortality¹. Left atrial (LA) remodeling, involving both structural and functional changes, plays a crucial role in the onset and persistence of AF². Even in patients with preserved left ventricular ejection fraction, AF-induced electrical and mechanical dyssynchrony can cause progressive LA dilation, fibrosis, and weakened contractility³. These alterations disrupt the normal atrial filling and emptying, further exacerbating the arrhythmia. Catheter ablation has become an effective treatment for restoring and maintaining sinus rhythm in AF patients. While many studies have shown its clinical effectiveness, the post-ablation temporal dynamics of LA reverse remodeling remain unclear. Understanding these dynamics is vital as it can offer insights into arrhythmia recurrence mechanisms and guide personalized management. Recent advancements in echocardiography, especially two-dimensional speckle-tracking imaging (2D-STI), have transformed the assessment of LA mechanics. As demonstrated in research published in JACC Cardiovascular Imaging, 2D-STI can precisely quantify LA strain and strain rate, detecting subtle atrial function changes⁴. There is a lack of longitudinal data on the post-ablation recovery p.a. tterns of LA stiffness and strain. Existing studies mainly focus on short-term outcomes or single-time point assessments, failing to capture the dynamic nature of LA remodeling over time⁵. This prospective study aims to using multi-parametric echocardiography to systematically evaluate the dynamic changes in LA structure, function, and stiffness in paroxysmal AF patients with preserved LVEF, we aim to reveal

Department of Cardiology, General Hospital of Northern Theater Command, No. 83 Wenhua Road, Shenhe District, Shenyang 110016, China. ✉email: mqiqi_chen@163.com

the characteristic patterns of LA reverse remodeling, identify predictors of arrhythmia recurrence, and provide evidence-based suggestions for post-ablation clinical follow-up.

Data and Methods

General information

Objects

This study enrolled 89 patients with paroxysmal atrial fibrillation (PAF) who underwent catheter ablation at our hospital from March 2023 to April 2024. Of these patients, 42 were male and 47 were female, with a mean age of 59.48 ± 8.91 years. Clinical data of patients were collected, and informed consent was obtained from all participants. All patients completed the full follow-up schedule, with no missing data.

Inclusion criteria

(1) Patients with a confirmed diagnosis of PAF (meeting the ESC/HRS guideline⁶ criteria, with atrial fibrillation episodes lasting < 7 days and terminating spontaneously); (2) Patients with a left ventricular ejection fraction (LVEF) of $\geq 50\%$ and no structural heart disease (e.g., hypertrophic cardiomyopathy, moderate or severe valvular disease); (3) Patients scheduled for first-time radiofrequency ablation (pulmonary vein isolation); (4) Patients aged 18–80 years who had signed an informed consent document.

Exclusion criteria

(1) Patients with valvular heart disease or those who have undergone valve replacement procedure; (2) Patients with a history of atrial fibrillation ablation; (3) Patients with congenital heart disease; (4) Patients showing thrombosis in the atrium or auricle during transesophageal echocardiography; (5) Patients with hyperthyroidism.

Instruments and Examination Methods *Instrument:* The Philips EPIQ7C ultrasound diagnostic device was used, with a transthoracic ultrasound probe model X5-1, frequency between 1 and 5 MHz, and a probe depth of 15–20 mm. The quantitative analysis software was QLAB10.5. Patients were positioned on the examination bed in the left lateral decubitus position and instructed to breathe calmly. Before the examination, limb lead electrocardiography was connected, and continuously collecting and storing clear dynamic images of three cardiac cycles for subsequent offline analysis. The patients' height and weight were recorded, and input into the ultrasound diagnostic instrument, and the system automatically calculated the body surface area (BSA).

Two - dimensional echocardiography In the parasternal long - axis view of the left ventricle, left atrial diameter (LAD) and left ventricular ejection fraction (LVEF) were measured. In the apical four-chamber view, left atrial appendage flow velocity (LAA-v) and the mitral valve early diastolic peak velocity (E peak) were measured. Also, in this view, Simpson's method was used to measure the left atrial end - diastolic volume (LAEDV), left atrial end - systolic volume (LAESV) (Fig. 1), left atrial presystolic volume (LAVp), and left atrial ejection fraction (LAEF).

Calculated the:

Left atrial active ejection fraction (LAAEF): $LAAEF = (LAVp - LAESV) / LAVp \times 100\%$.

Left atrial passive ejection fraction (LAPEF): $LAPEF = (LAEDV - LAVp) / LAEDV \times 100\%$.

Left atrial volume index (LAVI): $LAVI = LAEDV / BSA$.

2D-STI Acquired standard two - chamber and four - chamber views in the apical long-axis position, saving three consecutive cardiac cycles for each. Opened the QLAB10.5 quantitative analysis software, entered the aCMQ mode, selected TMAD, and imported the saved images. Placed fixed points at the left atrial apex and both sides of the mitral valve annulus. The system generated left atrial myocardial segmental strain curves. If the endocardium was unclear or incomplete, manually adjusted the fixed points until the endocardium was clearly displayed. Then, the peak left atrial systolic strain (LASRs), peak left atrial systolic strain rate (mLASRs), peak early left atrial diastolic strain (LASRe), peak early left atrial diastolic strain rate (mLASRe), peak late left atrial diastolic strain (LASRa) and late left atrial diastolic strain rate (mLASRa) were obtained, and data analysis was performed after getting the average values. This study takes the QRS wave of the electrocardiogram as the starting point, thus LASRs and mLASRs are positive values, while LASRe, mLASRe, LASRa, and mLASRa are negative values (Fig. 2).

TDI: In the apical four-chamber view, activated the TDI mode, placed the sampling points sequentially at the left atrial side and septal side of the mitral valve annulus. The early diastolic peak velocity of the septal side of the mitral valve annulus (septal e') and the early diastolic velocity of the left atrial side of the mitral valve annulus (left atrial e') were measure, then calculated the average value to get the early diastolic peak velocity of the mitral valve annulus (e'), and calculated the left atrial stiffness (LAsT) using the formula: $LAsT = (E/e') / LASRs$.

Ablation Procedure

During the procedure, a coronary sinus electrode catheter was inserted into the coronary sinus via the patient's internal jugular vein or left femoral vein, then a guidewire was placed in the superior vena cava through the right femoral vein, followed by the placement of a sheath over the guidewire, and a puncture needle was then inserted through the sheath for atrial septal puncture. Heparin was administered at a dose of 100 IU/kg during the procedure. The Pentaray multipolar mapping catheter was advanced into the left atrium via the sheath. Under the guidance of the CARTO 3D electrophysiological mapping system, structural reconstruction of the left atrium and bilateral pulmonary veins was performed. The radiofrequency output power was set at 35–40 W,

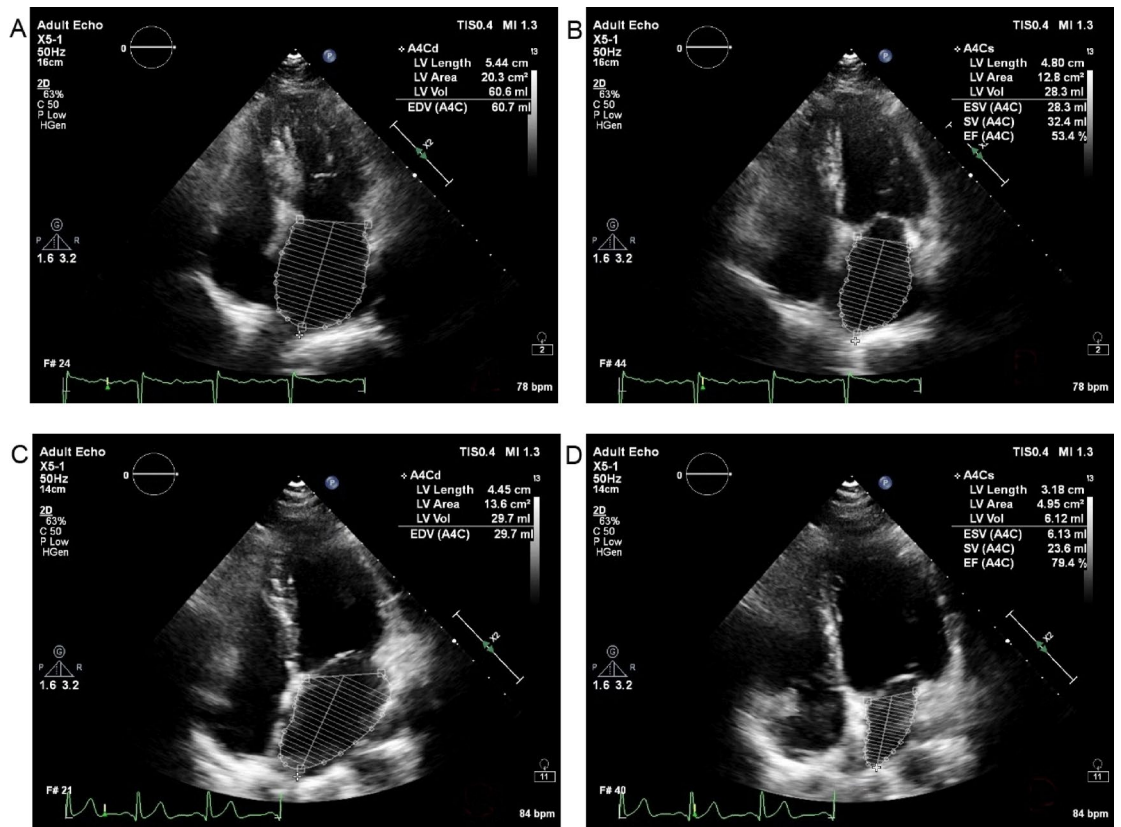


Fig. 1. Left atrial end-diastolic volume (A) and left atrial end-systolic volume (B) before catheter ablation; Left atrial end-diastolic volume (C) and left atrial end-systolic volume (D) three months after catheter ablation.

and the radiofrequency generator temperature at 43°C for ablation. The target was to achieve pulmonary vein isolation, with ablation duration adjusted based on tissue contact and impedance changes⁶.

Statistical analysis Data analysis was performed using SPSS 26.0. Count data were presented as cases or percentages and analyzed using the chi-square test. Normally distributed measurement data were expressed as mean \pm standard deviation ($\bar{X} \pm S$) and compared using the t-test. Non-normally distributed data were presented as median (interquartile range) and analyzed using the rank-sum test. $P < 0.05$ was considered statistically significant. To assess the predictive value of LA parameters for AF recurrence, a Cox proportional hazards model was used, with clinical follow-up for 12 months post-ablation.

Results

General information of patients

This study included 89 patients, with an average age of 59.48 ± 8.91 years, including 42 males, accounting for 47.19% (Table 1).

Comparison of left atrial structure and function parameters before and after catheter ablation procedure

One day after ablation, LVEF, LASRs, LASRe, LASRa, mLASRe, and mLASRa were lower than pre-ablation, while LAEF was higher ($P < 0.05$). One month post-ablation, LAD, LAEDV, LAESV, LAVp, LAsT, and LAVI were decreased compared with those before ablation, whereas LAA - V, LAEF, LVEF, LASRs, LASRe, LASRa, mLASRs, and mLASRe were increased ($P < 0.05$). Three months post-ablation, LAD, LAEDV, LAESV, LAVp, LAVI, and LAsT were decreased compared with those before ablation, and LAA - V, LAEF, LVEF, LASRs, LASRe, LASRa, mLASRs, mLASRe, and mLASRa were increased compared to pre-ablation ($P < 0.05$) (Table 2).

Cox regression analysis showed that the recovery rate of LASRs at 1 month post-ablation (Δ LASRs) was an independent predictor of AF recurrence (hazard ratio [HR] = 0.72, 95% confidence interval [CI]: 0.54–0.96, $P = 0.023$). Patients with Δ LASRs $< 10\%$ had a significantly higher recurrence rate than those with Δ LASRs $\geq 10\%$ (32.1% vs. 11.5%, $P = 0.014$).

Discussion

1 AF is one of the most common arrhythmias, with its incidence rising markedly with age⁷. This study systematically reveals the dynamic evolution patterns of left atrial structure, function, and stiffness after radiofrequency ablation in PAF patients who have normal ejection fractions via multi-time-point echocardiography, as well

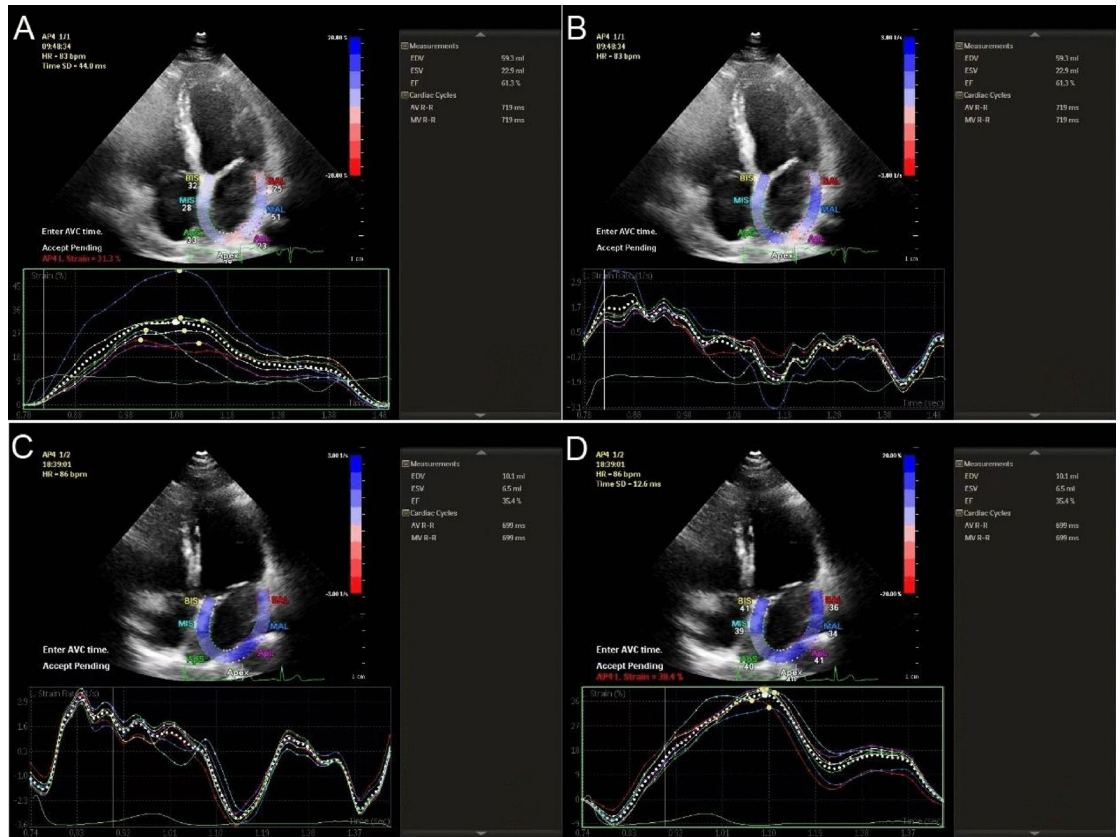


Fig. 2. left atrial strain (A) and strain rate (B) in the apical four-chamber view before catheter ablation; Left atrial strain (C) and strain rate (D) in the apical four-chamber view three months after catheter ablation.

Item	n = 89
Age (year)	59.48 ± 8.91
Male [n(%)]	42(47.19%)
Atrial fibrillation course (Month)	65.74 ± 52.13
History hypertension [n(%)]	46(51.68%)
History of coronary heart disease [n(%)]	7(7.86%)
History of diabetes [n(%)]	12(13.48%)
History of stroke or embolism [n(%)]	7(7.86%)
CHA2DS2- VASc score	1.91 ± 1.38
HAS-BLED score	1.06 ± 0.85

Table 1. Baseline data of patients.

as its clinical significance, which offer new insights into the mechanisms of atrial reverse remodeling and AF recurrence prediction.

2 Left atrial remodeling is an important pathological basis for the occurrence and maintenance of AF⁸. This study observed that the structure and function parameters of left atrium after radiofrequency ablation showed a characteristic time-dependent change pattern. In the early postoperative stage, significant changes in left atrial function occurred, manifested as reduced strain parameters and increased stiffness, possibly reflecting acute myocardial injury and inflammatory responses caused by ablation⁸. The transient decrease in LASRs (12.7% reduction) at 1 day post-ablation aligns with previous findings of acute myocardial stunning after thermal ablation⁹. Notably, recent advancements in ablation technology have introduced pulsed field ablation (PFA) as a novel strategy. Studies have shown that PFA may offer distinct advantages in preserving left atrial compliance compared to traditional thermal ablation techniques. A recent publication in JACC Clinical Electrophysiology highlighted that PFA is associated with a significantly lower risk of stiff left atrial syndrome, potentially due to its non-thermal mechanism of action that minimizes tissue fibrosis and structural damage¹⁰. This finding is particularly relevant as our study demonstrates that LA stiffness (LAST) recovery post-ablation is closely linked to clinical outcomes. While our cohort exclusively underwent radiofrequency ablation, the emerging evidence on

Variable	Before ablation	1 day after ablation	1 month after ablation	3 month after ablation
LAD (mm)	38.24 ± 4.22	37.92 ± 3.92	36.14 ± 3.60#	34.89 ± 2.61△
LAEDV (mm)	46.44 ± 7.69	44.05 ± 10.21	42.56 ± 7.99#	35.98 ± 5.66△
LAESV (mm)	23.67 ± 6.17	21.99 ± 6.02	21.28 ± 5.01#	18.20 ± 4.17△
LAVp (mm)	33.20 ± 6.80	32.88 ± 7.86	30.65 ± 6.09#	26.02 ± 4.70△
LAVI (ml/m ²)	25.49 ± 4.79	24.21 ± 5.85	23.51 ± 5.11#	19.82 ± 3.76△
LAA-V (cm/s)	0.36 ± 0.08	0.37 ± 0.07	0.45 ± 0.05#	0.50 ± 0.07△
LAEF (%)	0.50 ± 0.09	0.53 ± 0.07*	0.55 ± 0.07#	0.55 ± 0.06△
LVEF (%)	0.57(0.60)	0.56(0.59)*	0.58(0.61)#	0.61(0.64)△
LAAEF (%)	0.28 ± 0.10	0.31 ± 0.08	0.30 ± 0.08	0.30 ± 0.07
LAPEF (%)	0.27(0.32)	0.26(0.32)	0.25(0.33)	0.26(0.32)
LASRs (%)	19.76 ± 2.40	17.25 ± 2.59*	22.83 ± 2.23#	26.91 ± 2.59△
LASRe (%)	-10.37 ± 1.46	-9.30 ± 1.71*	-11.80 ± 1.42#	-12.97 ± 1.85△
LASRa (%)	-9.39 ± 1.94	-7.95 ± 1.93*	-11.02 ± 2.05#	-13.93 ± 2.46△
mLASRs (S ⁻¹)	0.67 ± 0.09	0.66 ± 0.10	0.85 ± 0.11#	1.03 ± 0.27△
mLASRe (S ⁻¹)	-0.75 ± 0.08	-0.64 ± 0.13*	-0.83 ± 0.10#	-1.07 ± 0.21△
mLASRa (S ⁻¹)	-0.81 ± 0.15	-0.71 ± 0.11*	-0.85 ± 0.13	-0.86 ± 0.12
LASSt	0.49 ± 0.09	0.52 ± 0.12	0.40 ± 0.09#	0.31 ± 0.07△

Table 2. Changes of left atrial structure and function parameters before and after catheter ablation procedure. Note: $P < 0.05$ vs. pre-ablation; # $P < 0.05$ vs. pre-ablation; △ $P < 0.05$ vs. pre-ablation.

PFA's effects on LA mechanics warrants future investigation. Comparative studies between ablation modalities—specifically evaluating their impact on LA strain, stiffness, and long-term reverse remodeling—could further refine personalized treatment strategies for PAF patients¹⁰. Notably, left atrial structural parameters had not shown significant changes at this point, indicating that functional abnormalities may occur before structural alterations. As time went by, one month after the operation, there was an obvious reverse remodeling of the left atrium, shown as the continuous improvement of structural parameters and the gradual recovery of function, and this time-dependent change pattern provided important clues for understanding the reversibility of atrial remodeling¹¹.

3 The early increase in LAEF (53.0% at 1 day post-ablation) deserves specific discussion. This may be attributed to compensatory mechanisms, such as reduced left atrial presystolic volume (LAVp) and improved ventricular diastolic function. The maintenance of LAEF despite decreased strain parameters suggests a transient adjustment in atrial-ventricular coupling, which warrants further investigation in future studies.

4 In terms of the predictive value of AF recurrence, this study found that the dynamic changes of left atrial stiffness and strain parameters had important clinical significance. The increase in stiffness in the early postoperative period may reflect the degree of myocardial injury¹², while the subsequent sustained improvement suggests an effective reverse atrial remodeling process¹³. Notably, the recovery rate of LASRs at 1 month post-ablation emerged as a robust predictor of long-term outcomes, which is consistent with prior research showing that LA strain recovery correlates with sinus rhythm maintenance¹⁴. The observed HR of 0.72 for ΔLASRs indicates that each 10% increase in strain recovery reduces the recurrence risk by 28%, highlighting its clinical utility.

5 The dynamic evolution of left atrial structural and functional parameters may stem from multiple mechanisms¹⁵. Restored sinus rhythm reduces atrial volume and pressure load, creating conditions for reverse remodeling. Ablation may break the vicious cycle of electrical and structural remodeling by removing AF triggers and improving atrial substrate¹⁶. In addition, the regression of the inflammatory response¹⁷ and the initiation of the myocardial repair process jointly promote the gradual recovery of atrial function¹⁸. These mechanisms work together and eventually lead to the continuous improvement of structure and function of the left atrium¹⁹.

6 From the perspective of clinical application, the results of this study support the inclusion of the dynamic assessment of left atrial structure and function into the postoperative follow-up system. By monitoring the changes of parameters at specific times points, clinicians can evaluate the ablation effect and predict prognosis more accurately²⁰. Especially, the time-independent change pattern of left atrial stiffness and strain parameters may provide important references for individualized treatment decisions²¹. For patients with suboptimal parameter improvement, early intervention and enhanced follow-up may contribute to improving the long-term prognosis.

7 Notably, the RFA procedure in this study utilized a standardized power setting of 35–40 W with a target temperature of 43 °C, consistent with conventional thermal ablation protocols for pulmonary vein isolation. However, we did not employ ablation index (AI) or contact force guidance, which are increasingly recognized as tools to optimize lesion transmural and reduce complications⁹. Recent data from Europace highlighted that power settings significantly influence ablation efficacy in the left atrial posterior wall—specifically, higher power (40 W) achieved more consistent transmural isolation compared to lower settings (30 W), albeit with a slightly increased risk of collateral damage⁹. This aligns with our observation that LA strain parameters (e.g., LASRs) showed transient impairment at 1 day post-ablation, potentially reflecting acute thermal injury to atrial

myocardium, particularly in the posterior wall where tissue thickness and proximity to adjacent structures may amplify energy effects.

8 In contrast, the absence of AI guidance means our approach relied on impedance monitoring and procedural experience to adjust lesion duration (typically 30–60 s per point), which may introduce variability in lesion quality. Future studies comparing AI-guided vs. conventional RFA could clarify whether standardized lesion parameters further enhance LA reverse remodeling, as more uniform transmural ablation might reduce residual atrial substrate and accelerate functional recovery. The correlation between posterior wall ablation power and LA stiffness recovery—observed in our 1-month follow-up data—merits exploration, as optimized energy delivery to this region may be critical for preserving atrial compliance and reducing recurrence risk¹⁰.

9 It is important to acknowledge several limitations of this study. First, the study cohort included only patients who underwent radiofrequency ablation, and the findings may not be generalizable to other ablation modalities such as cryoballoon or pulsed field ablation (PFA). Recent data have highlighted that PFA may preserve left atrial compliance more effectively than thermal ablation, which is an important consideration for future comparative studies²². Second, the baseline characteristics lacked detailed assessment of AF burden (e.g., attack frequency, duration), which could influence LA remodeling dynamics. Third, the follow-up period was limited to 3 months, and long-term data on the persistence of LA reverse remodeling are needed.

10 In summary, following radiofrequency ablation, the left atrium undergoes characteristic dynamic changes in structure, function, and stiffness. Study results suggest that: (1) A temporary drop in left atrial function within 1 day post-ablation is a normal physiological response and should not be over-interpreted as procedural failure; (2) The 1-month post-procedure evaluation is highly predictive of long-term surgical outcomes, with LASRs recovery rate serving as a key biomarker; (3) Left atrial strain parameters, particularly LASRs, are more sensitive than traditional parameters for assessing left atrial function. These findings provide an important basis for the clinical assessment of procedural outcomes and prognosis, and support incorporating 2D speckle tracking imaging into routine follow-up protocols.

Conclusion

10 This study systematically evaluates the dynamic changes in left atrial (LA) structure and function after catheter ablation in paroxysmal atrial fibrillation (PAF) patients using conventional echocardiography and 2D speckle-tracking imaging (2D-STI). The key findings reveal that LA reverse remodeling follows a characteristic pattern of “functional recovery preceding structural recovery”. LA strain parameters transiently decreased at 1 day post-ablation, with structural and functional improvements observed from 1 month onward. The recovery rate of LA strain at 1 month is an independent predictor of atrial fibrillation recurrence. Multi-modal echocardiography, especially 2D-STI, effectively monitors these dynamic changes. Clinically, evaluating LA functional parameters at 1 month post-procedure aids in predicting long-term prognosis and guiding personalized follow-up.

Data availability

All data generated or analysed during this study are included in this published article.

Received: 21 May 2025; Accepted: 21 July 2025

Published online: 02 August 2025

References

1. January, C. T. et al. 2014 AHA/ACC/HRS guideline for the management of patients with atrial fibrillation: a report of the American college of cardiology/american heart association task force on practice guidelines and the heart rhythm society. *J. Am. Coll. Cardiol.* **64** (21), e1–e76 (2014).
2. Allesie, M., Ausma, J. & Schotten, U. Electrical, contractile and structural remodeling during atrial fibrillation. *Cardiovasc. Res.* **54** (2), 230–246 (2002).
3. Valderrabano, M. et al. Left atrial function in patients with atrial fibrillation and preserved ejection fraction: a systematic review and meta-analysis. *J. Am. Soc. Echocardiogr.* **32** (8), 921–934 (2019).
4. Mălăescu, G. G. et al. Left atrial strain determinants during the cardiac phases. *JACC Cardiovasc. Imaging.* **15** (3), 381–391 (2022).
5. Bajraktari, G., Bytyçi, I. & Henein, M. Y. Left atrial structure and function predictors of recurrent fibrillation after catheter ablation: a systematic review and meta-analysis. *Clin. Physiol. Funct. Imaging.* **40** (1), 1–13 (2020).
6. Aldaas, O. M. et al. Pulsed field ablation versus thermal energy ablation for atrial fibrillation: a systematic review and meta-analysis of procedural efficiency, safety, and efficacy. *J. Interv Card Electrophysiol.* **67** (3), 639–648 (2024).
7. Hindricks, G. et al. 2020 ESC guidelines for the diagnosis and management of atrial fibrillation developed in collaboration with the European association for Cardio-Thoracic surgery (EACTS): the task force for the diagnosis and management of atrial fibrillation of the European society of cardiology (ESC) developed with the special contribution of the European heart rhythm association (EHRA) of the ESC. *Eur. Heart J.* **42** (5), 373–498 (2021).
8. Schwab, A. C. et al. Rhythm monitoring, success definition, recurrence, and anticoagulation after atrial fibrillation ablation: results from an EHRA survey. *Europace* **25** (2), 676–681 (2023).
9. Smith, A. J. et al. Comparative effects of different power settings for achieving transmural isolation of the left atrial posterior wall with radiofrequency energy. *Europace* **26** (11), euae265. <https://doi.org/10.1093/europace/euae265> (2024).
10. Aldaas, O. M. et al. Pulsed field ablation versus thermal energy ablation for atrial fibrillation: a systematic review and meta-analysis of procedural efficiency, safety, and efficacy. *J. Interv Card Electrophysiol.* **67** (3), 639–648. <https://doi.org/10.1007/s10840-024-01072-3> (2024).
11. Hammerstingl, C. et al. Left atrial deformation imaging with ultrasound based two-dimensional speckle-tracking predicts the rate of recurrence of paroxysmal and persistent atrial fibrillation after successful ablation procedures. *J. Cardiovasc. Electrophysiol.* **23** (3), 247–255 (2012).
12. Cho, D. H. et al. Atrial cardiomyopathy with impaired functional reserve in patients with paroxysmal atrial fibrillation. *J. Am. Soc. Echocardiogr.* **36** (2), 180–188 (2023).
13. Moon, I. et al. Extensive left atrial ablation was associated with exacerbation of left atrial stiffness and dyspnea. *J. Cardiovasc. Electrophysiol.* **30** (12), 2782–2789 (2019).

14. Kishima, H. et al. Left atrial ejection force predicts the outcome after catheter ablation for paroxysmal atrial fibrillation. *J. Cardiovasc. Electrophysiol.* **29** (2), 264–271 (2018).
15. Wijesurendra, R. S. & Casadei, B. Mechanisms of atrial fibrillation[J]. *Heart* **105** (24), 1860–1867 (2019).
16. Walek, P. et al. Echocardiographic assessment of left atrial morphology and function to predict maintenance of sinus rhythm after electrical cardioversion in patients with non-valvular persistent atrial fibrillation and normal function or mild dysfunction of left ventricle[J]. *Cardiol. J.* **27** (3), 246–253 (2020).
17. Hisazaki, K. et al. Endothelial damage and thromboembolic risk after pulmonary vein isolation using the latest ablation technologies: a comparison of the second-generation cryoballoon vs. contact force-sensing radiofrequency ablation[J]. *Heart Vessels.* **34** (3), 509–516 (2019).
18. Kirchhof, P. et al. Early rhythm-control therapy in patients with atrial fibrillation[J]. *N. Engl. J. Med.* **383** (14), 1305–1316 (2020).
19. Laish-Farkash, A. et al. Evaluation of left atrial remodeling by 2D-speckle-tracking echocardiography versus by high-density voltage mapping in patients with atrial fibrillation. *J. Cardiovasc. Electrophysiol.* **32** (2), 305–315 (2021).
20. Relander, A. et al. Advanced interatrial block predicts ineffective cardioversion of atrial fibrillation: a FinCV2 cohort study. *Ann. Med.* **53** (1), 722–729 (2021).
21. Brás, P. G. et al. Evaluation of left atrial strain imaging and integrated backscatter as predictors of recurrence in patients with paroxysmal, persistent, and long-standing persistent atrial fibrillation undergoing catheter ablation. *J. Interv Card Electrophysiol.* **67** (3), 479–492 (2024).
22. Kim, J. A. & Chelu, M. G. Comparison of cryoballoon and radiofrequency ablation for persistent atrial fibrillation: a systematic review and meta-analysis. *J. Interv Card Electrophysiol.* **66** (3), 585–595 (2023).

Author contributions

Liu NN: conceived and designed the experiments, performed the experiments. Zhang Q and Sun JS: performed the experiments, analyzed the data, and wrote the manuscript. Li GS and Wang MY: collected the data; Wang ZL and Liang M and Su YX: analyzed the data and proofed the manuscript. All authors have proofed the article.

Declarations

Competing interests

The authors declare no competing interests.

Ethics approval

The study has been approved by the ethics committee of General Hospital of Northern Theater Command. All methods were performed in accordance with the relevant guidelines and regulations.

Conflict of interest

The authors declare that there is no conflict of interest.

Additional information

Correspondence and requests for materials should be addressed to N.N.L.

Reprints and permissions information is available at www.nature.com/reprints.

Publisher's note Springer Nature remains neutral with regard to jurisdictional claims in published maps and institutional affiliations.

Open Access This article is licensed under a Creative Commons Attribution-NonCommercial-NoDerivatives 4.0 International License, which permits any non-commercial use, sharing, distribution and reproduction in any medium or format, as long as you give appropriate credit to the original author(s) and the source, provide a link to the Creative Commons licence, and indicate if you modified the licensed material. You do not have permission under this licence to share adapted material derived from this article or parts of it. The images or other third party material in this article are included in the article's Creative Commons licence, unless indicated otherwise in a credit line to the material. If material is not included in the article's Creative Commons licence and your intended use is not permitted by statutory regulation or exceeds the permitted use, you will need to obtain permission directly from the copyright holder. To view a copy of this licence, visit <http://creativecommons.org/licenses/by-nc-nd/4.0/>.

© The Author(s) 2025